WOOD RESEARCH doi.org/10.37763/wr.1336-4561/68.1.183199
ISSN 1336-4561 e-ISSN 2729-8906
68(1): 2023 183-199 pp.

QUALITY EVALUATION OF UHF RFID ANTENNAS AND PASSIVE TAGS ON PAPER SUBSTRATES

JURAJ GIGAC, MÁRIA FIŠEROVÁ, SVETOZÁR HEGYI, MAROŠ KOVÁČ
PULP AND PAPER RESEARCH INSTITUTE
SLOVAK REPUBLIC

(RECEIVED SEPTEMBER 2022)

ABSTRACT

The effect of antenna design modification, paper substrates and relative electrical permittivity of background materials on the reflection coefficient of UHF RFID antennas was studied. Simulation software was used to modify the design and calculate the reflection coefficient of the antennas. By modifying the coupling of the dipole with the induction loop of the antennas, a reduction of the simulated reflection coefficient was achieved compared to the commercial antenna. The positive effect of antenna modification was also confirmed by measuring the reflection coefficient of antennas printed on paper by thermal transfer printing, placed on extruded polystyrene and particle board. The reflection coefficient of the modified antennas was lower when placed on extruded polystyrene, whose relative electrical permittivity was lower than particle board. After installing the memory chip to the antennas printed on paper and paperboard, the identification, reading and recording range of passive UHF RFID tags were measured after they were placed on thicker paperboard, extruded polystyrene and particle board. The positive effect of antenna modification on improving the communication quality of passive UHF RFID tags placed on background materials with a relative electrical permittivity of 2.4 to 6.7 was confirmed.

KEYWORDS: Paper, simulation, design, antenna, reflection coefficient, tag, communication.

INTRODUCTION

Radio Frequency Identification (RFID) is a technology that enables wireless short- and medium-range tracking and identification of objects. Basic RFID systems are mainly composed of two entities, namely reader and tag. Reader broadcasts queries to the tag in its wireless transmission range for information contained in tag, this last will reply with the required information. RFID tags can be active, with an on-board power supply such as a battery, or

passive, harvesting their energy from the RF signal sent by the reader. RFID systems can be designed to operate in a variety of frequency bands, depending on the transmission distance and data rate required for the application. There are two conditions that must be fulfilled for a reader to communicate with a RFID tag. The first condition is sufficient gain to activate the tag, and the second condition is that the power reflected by the tag is high enough for the reader to detect it. This performance is degraded not only by the distance and obstacles between the reader and the tag, but also by the material (plastic, paper, cardboard, wood, water, ethylene glycol, beef, metal) on which the tag is placed (Griffin et al. 2005).

Printed electronics facilitates the fabrication of next-generation electronics through conventional printing methods, providing a simple and scalable strategy for fabricating low-cost, thin, lightweight, and flexible devices. Printing methods have been used successfully to fabricate devices such as intelligent labels, smart packaging, printed sensor systems, batteries, solar cells, antennas, and light-emitting devices (Shrestka et al. 2021, Sowade et al. 2019, Kim et al. 2019, Salmerón et al. 2014, An 2019, Zhang et al. 2013, Wang et al. 2020).

Plastic substrates used in printed electronics, such as polyethylene terephthalate (PET), polyimide (PI) and polyethylene naphthalate (PEN), are produced from non-renewable petrochemicals, which contribute to the climate change crisis. At the end of life, most plastics end up in landfills, with less than a third of plastic waste generated globally being recycled (Geyer et al. 2017).

Paper substrates have not yet replaced plastics in many applications, because the porous microstructure of paper causes the imbibition and wicking of functional inks, which compromises printability and resolution (Shrestha et al. 2021, Sowade et al. 2019, Kim et al. 2019, Salmerón et al. 2014, An 2019, Zhang et al. 2013, Wang et al. 2020). Furthermore, an ideal green process for end-of-life recycling should separate and reuse electronic materials and recycle the substrate. Although paper is recycled more than PET, the absorption of functional inks into paper makes it more difficult to separate electronic materials from paper than from PET (Wäger et al. 2005, Aliaga et al. 2015, Li et al. 2004, Glogic et al. 2021, Mishra et al. 2021).

Paper has a rougher surface compared to plastic film. Irregular surfaces and structural properties of conventional papers require higher ink consumption, allowing them to be used only for electronic components with lower resolution or print quality requirements. In order to improve printability, research of paper substrates is aimed at improving surface smoothness and absorption properties. Coating and smoothing processes in a calender or hot stamping machine can be used to finish the surface of the paper (Gigac and Fišerová 2022). The paper surface is usually smoothed with a dispersion coating consisting of mineral pigments and organic binders. The smoothness of the paper surface depends on composition of coatings, the amount and layers of the coating and the final surface finish. The surface properties can be adjusted at the same time to achieve the desired functional properties, such as water, oil and grease resistance, low vapour and gas permeability (Long et al. 2015, Brodnjak and Todorova 2017, Ilyas et al. 2018, Kopačič et al. 2018, Gigac et al. 2018), and flame retardation (Sonnier et al. 2018).

Printing methods for antennas include screen printing, flexography, gravure, inkjet and thermal transfer. Various plastic films (Chin et al. 2008, Janeczek 2010, Arazna et al. 2017) or, less commonly, paper substrates (Merilampi et al. 2007, Rida et al. 2009, Lakafosis et al. 2010,

Xi et al. 2011, Zichner and Baumann 2011, Öhlund and Anderson 2012, Bolström and Toivakka 2013, Kavčič et al. 2014, He et al. 2016) are used to print antennas. Thermal transfer printing with Metallograph® conductive ribbon is a simple, fast and economical method of digital printing for electronic circuits, sensors and RFID antennas (Taylor 2017, Taylor and Harrison 2017). Metallograph® ribbon, a product of IIMAK and SPF-Inc. comprising a heat-resistant coating, a carrier polyethylene terephthalate (PET) film, a release layer, a vacuum metallised continuous layer, and a thermoplastic bonding layer that bonds the metallised layer to the substrate when heated in the thermal transfer printer. Compared to printing techniques such as screen printing, flexography, gravure and inkjet printing, which use pastes and inks containing mostly silver nanoparticles, thermal transfer printing uses aluminum, which is about two orders of magnitude less costly for the equivalent conductivity of silver. Additionally, there are no fluids, no printing set up, no drying and no sintering of the silver nanoparticles. Without these additional steps the process has a very small footprint and takes less than a second to accomplish.

Dipole antennas are the simplest form of antenna and are extensively used for transmitting and receiving radio frequency signals. Due to their excellent directional properties, dipole antennas are regularly used in radio and telecommunication systems as well as systems handling ultra-wideband signals. In a dipole antenna, feed point impedance plays a significant role in establishing good dipole characteristics. The tag antenna is the key component, it consists of a dipole, an induction loop and a connecting part. It must be properly designed to work well with the pad to which it is attached. It is very important to design the tag antenna to meet the transmitted power requirements in use. The length and thickness of the dipole arm determine the main characteristics of the antenna. The resonance of the tag antenna determines the performance and largely depends on relative electrical permittivity, magnetic permeability and thickness of the substrate on which the antenna is placed.

A passive UHF RFID tag placed on a conductive plane or water surface tends to suffer a lot. Many designs such as microstrip antenna and ferrite antenna have been used to solve this metal-water problem. Artificial magnetic materials such as ferrites can be used to increase gain and reduce the size of antennas because, unlike naturally occurring dielectrics, they have negative permeability (Stergiou et al. 2012, Kaur et al. 2015). The electromagnetic band gap (EBG) material which exhibits a unique forbidden band gap at certain frequency offers a potential solution to solve the problem of background materials effects. The dipole RFID antenna above three-layer mushroom like EBG material exhibited a good antenna gain and long read range. However, the complicated structure and high material cost greatly limit the application of tag. The authors (Gao and Yuen 2008) developed a new type of EBG material which uses a ferrite film to reduce the size and lower forbidden frequency.

Antenna design at all levels strongly relies on electromagnetic simulation software. However, despite the large number and the high quality of the available open-source simulation packages, most companies have no doubts about the choice of commercial program suites. At the same time, in the academic world, it is frequent to develop in-house simulation software, even from scratch and without proper knowledge of the existing possibilities. In this fast-growing background, the use and the development of numerical software for electromagnetic simulation follow in the industrial and academic world. The development of software for electromagnetic

simulation is in development, as evidenced by many recent articles (García et al. 2019, Taggar et al. 2019, Fedeli et al. 2017, Zhang et al. 2019).

The aim of the work was to determine the influence of the design of UHF RFID antennas on the reflection coefficient using simulation software. Comparison of measured reflection coefficients of antennas printed on paper, placed on different background materials. Evaluation of the effect of relative electrical permittivity and thickness of paper substrates as well as background materials on the communication quality of experimentally prepared passive tags.

MATERIAL AND METHODS

Materials

Tab. 1 shows materials for printing antennas, background materials for simulation and measurement of antennas reflection coefficients and for measuring the communication quality of passive UHF RFID tags. The electrical characteristics of the materials used are also listed.

Tab.1: Materials and their characteristics.

Materials for printing antennas					
Code	**Type**	**Grade**	**Electrical permittivity ε_r**	**Tan δ**	**Thickness (μm)**
P	Coated paper	Thermal transfer paper, experimental	2.8	0.008	75
PB1	Coated paperboard	GC2, Metsä Board	3.3	0.012	290
AL	Aluminum	Metallograph ribbon, SPF-Inc.	1.0	-	0.26
Background materials in the simulation and measurement of the reflection coefficient S11					
Code	**Type**	**Grade**	**Electrical permittivity ε_r**	**Tan δ**	**Thickness (mm)**
P	Coated paper at simulation		2.8	0.008	0.075
AIR	Free space at simulation		1.0	-	≥ 40
STYR	Extruded polystyrene	Styrodur 3000 CS, BASF	2.4	0.0002	40
MFPB	Work top of particle board	Melamine faced particle board, Kronospan	6.7	-	38
Background materials in the measurement of the tag communication					
Code	**Type**	**Grade**	**Electrical permittivity ε_r**	**Tan δ**	**Thickness (mm)**
PB2	Coated paperboard	GZ, Invercote Duo, Holmen Iggesund	3.5	0.012	1.0
STYR	The same materials as when measuring the reflection coefficient				
MFPB					

UHF RFID antennas – commercial COMM, modified MOD1 and MOD2 antennas were printed with an aluminum layer of thickness 0.26 μm on paper P and paperboard PB1. IC chip NXP UCODE G2iM+ (NXP Semiconductors, Netherlands) was used to prepare passive UHF RFID tags. Experimental passive UHF RFID tags – TCOMM_P, TMOD1_P, TMOD2_P, TCOMM_PB1, TMOD1_PB1, TMOD2_PB1 were used.

Methods

Simulations of the design and reflection coefficient of UHF RFID antennas in the free space (air) using the electromagnetic simulation software SONNET Suites 8.0, which allowed to define the design and material parameters of the antenna as well as the background materials (relative electrical permittivity ε_r, dielectric loss tangent δ, thickness).

Printing of UHF RFID antennas on paper and paperboards was carried out in a SATO thermal transfer printer SATO CL4NX (Japan) with Metallograph ribbon (SPF-Inc., USA).

Measurement of voltage standing wave ratio (VSWR) of the printed antennas was done using a symmetrization member (balun), which ensured the symmetrization of the line so as not to significantly affect the radiation characteristics of the antenna. Otherwise, the radiated energy of the antenna would be reduced which would result in reduction of the antenna gain. The measurement of the voltage standing wave ratio VSWR of the UHF RFID antennas was carried out after placing on top of 40 mm thick extruded polystyrene STYR as well as of 38 mm thick work top of particle board MFPB.

Reflection coefficient *S11* of the printed antennas was calculated from the measured voltage standing wave ratio (VSWR) according to the equation:

$$S11(dB) = 20.\log [(VSWR-1)/(VSWR+1)] \quad (1)$$

Preparation of UHF RFID tags was carried out by connecting two pins of the integrated circuit of the chip to the terminals of the inductive loop of the antenna using an isotropic conductive adhesive.

RESULTS AND DISCUSSION

Simulation of design and reflection coefficient of UHF RFID antennas

The simulation software SONNET was used to modify the design of the commercial UHF RFID COMM antenna and calculate the simulated reflection coefficients of the antennas. Two modified antennas MOD1 and MOD2 were prepared by simulation. The software allows insertion of antenna structures in drawing exchange format (DXF), subsequent modification of the antenna design in a very powerful graphic editor and its analysis. It is possible to simulate the material of the antenna and the background as well as their electrical parameters (relative electrical permittivity ε_r and dielectric loss tangent δ).

The design of the commercial antenna COMM with dimensions of 94 x 24 mm is shown in Fig. 1. Figs. 2 and 3 represent designs of modified antennas MOD1 and MOD2 obtained by modifying the coupling between the dipole and the induction loop of the commercial antenna COMM. The dimensions of the antennas in Figs. 1-3 are not in actual size and the coupling between the dipole and the induction loop is marked with an ellipsis. The UHF RFID antennas were designed to be connected to the chip at the 170-180 μm gap location at the terminals of the induction loop and meet the requirements for transmitted power.

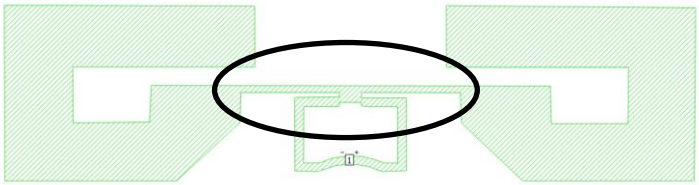

Fig. 1: Design of commercial antenna COMM (coupling length between the dipole and the induction loop is 3.15 mm, the width of the connection between the dipole and the induction loop is 0.65 mm).

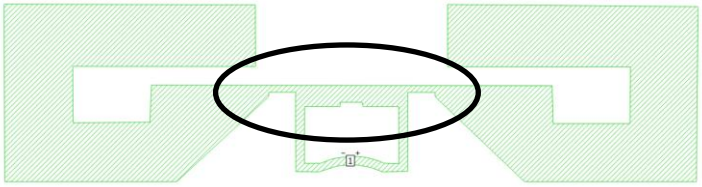

Fig. 2: Design of modified antenna MOD1 (coupling length between the dipole and the induction loop is 14.94 mm, the width of the connection between the dipole and the induction loop is 2.57 mm, the diagonal of the dipole is partially prolongated at the creation of the rebound).

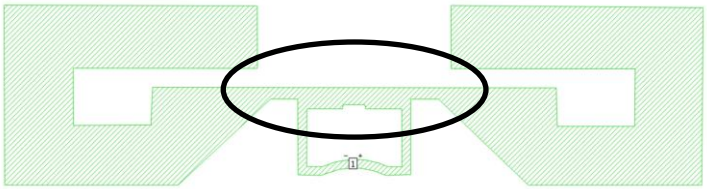

Fig. 3: Design of modified antenna MOD2 (coupling length between the dipole and the induction loop is 14.94 mm, the width of the connection between the dipole and the induction loop is 2.57 mm, the diagonal of the dipole is partially prolongated and the rebound is filled out).

Based on the reflection coefficient, it is possible to determine the quality of impedance customization of UHF RFID antennas, which has a significant impact on the correct function of the tag and directly affects the distance at which we can read the tag. The simulated reflection coefficient was determined using SONNET software. The influence of antenna design on the simulated reflection coefficient of UHF RFID antennas (COMM, MOD1, MOD2) on paper P surrounded by free space (AIR) depending on the frequency is presented in Fig. 4. A sharp decrease in the simulated reflection coefficient of all three antennas can be observed in the region resonance frequency f_{res}, which means an increase in the gain of the antenna and the reading range of passive UHF RFID tags.

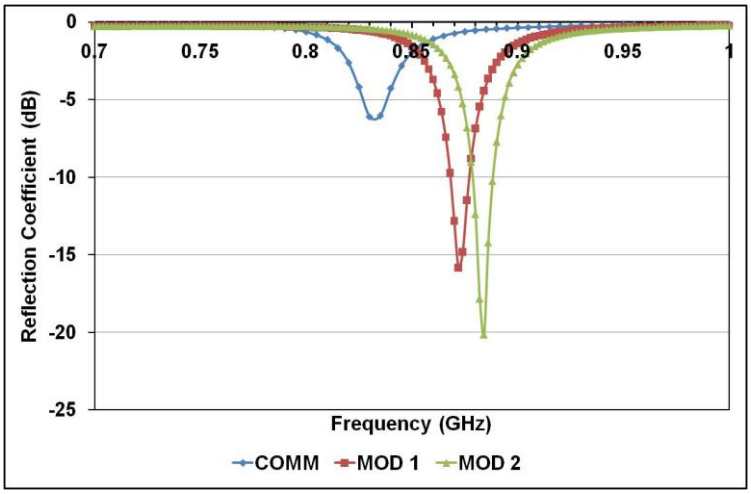

Fig. 4: Simulated reflection coefficient of commercial antenna COMM, modified antennas MOD1 and MOD2 on paper P surrounded by free space, versus frequency.

From the result of the simulation of the reflection coefficient of the commercial antenna COMM in the frequency range of 700-1000 MHz in Fig. 4, it can be concluded that the antenna provides a reflection coefficient of -6.1 dB at a relatively low resonance frequency f_{res} of 830 MHz. Modified antennas MOD1 and MOD2 had lower reflection coefficients at a higher resonance frequency f_{res}. The minimum value of the reflection coefficient of the modified antenna MOD1 was -15.8 dB at 872 MHz and antenna MOD2 -20 dB at 884 MHz frequency (Tab. 2).

Tab. 2: Simulated reflection coefficient of antennas lineup at resonance frequency.

Simulator	Antenna lineup*	Reflection coefficient S11 (dB)	Frequency f_{res} (MHz)
SONNET	COMM_P_AIR	-6.1	830
	MOD 1_P_AIR	-15.8	872
	MOD 2_P_AIR	-20.0	884

*Antennas on paper P surrounded by free space (AIR).

Measurement of the reflection coefficient of UHF RFID antennas

The commercial UHF RFID antenna COMM and modified antennas MOD1 and MOD2 were printed on paper P by thermal transfer printing using aluminum ribbon. The functionality of the antennas was evaluated by the reflection coefficient, which was calculated from the measured voltage standing wave ratio (VSWR). The influence of the antenna design and the background materials (extruded polystyrene STYR and particle board MFPB) used in the VSWR measurement on the antenna reflection coefficient was compared.

Fig. 5 depicts the course of the measured reflection coefficient of UHF RFID antennas (COMM, MOD1 and MOD2) printed on P paper, placed on extruded polystyrene STYR and on particle board HFPB, as a function of frequency.

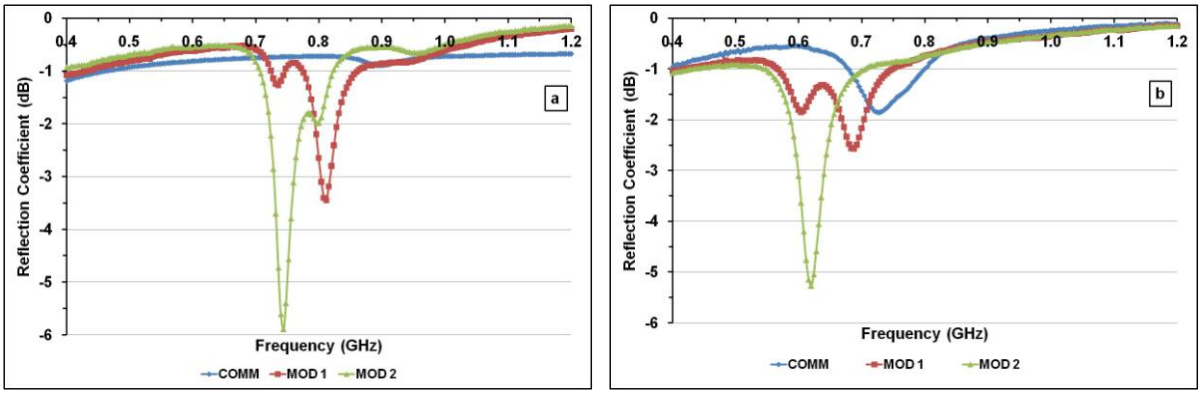

Fig. 5: Measured reflection coefficient of the commercial antenna COMM and modified antennas MOD1 and MOD2 printed on paper P, placed on extruded polystyrene STYR (a) and particle board HFPB (b), versus frequency.

From the measurements of the reflection coefficients in the frequency range 400-1200 MHz (Fig. 5), it follows that the modified antenna MOD2 had the lowest reflection coefficients of -5.9 dB at 744 MHz resonance frequency when it was placed on extruded polystyrene STYR and on particle board MFPB -5.3 dB at 620 MHz resonance frequency. The modified antenna MOD1 placed on STYR or MFPB materials also had lower reflection coefficients than the commercial antenna COMM. Antennas placed on STYR extruded polystyrene had lower reflection coefficients at higher resonance frequencies compared to antennas placed on particle board MFPB (Tab. 3).

Tab. 3: Measured reflection coefficient of antennas lineup at resonance frequency.

	Antenna lineup*	**Reflection coefficient S11 (dB)**	**Frequency f_{res} (MHz)**
Measurement	COMM_P_STYR	-2.0	1090
	MOD 1_P_STYR	-3.5	812
	MOD 2_P-STYR	-5.9	744
	COMM_P_MFPB	-1.9	728
	MOD 1_P_MFPB	-2.6	688
	MOD 2_P_MFPB	-5.3	620

*Antennas printed on paper P placed on extruded polystyrene STYR or particle board MFPB.

Fig. 6 presents the measured values of the reflection coefficients of the antennas (COMM, MOD1, MOD2) printed on paper P and placed on extruded polystyrene STYR and particle board HFPB at 865 MHz frequency. Antennas placed on extruded polystyrene STYR had a lower reflection coefficient than antennas placed on particle board MFPB. The reason is a significant difference in relative electrical permittivity of extruded polystyrene STYR (2.4) and particle board MFPB (6.7). The positive effect of the modification of the commercial antenna COMM was manifested mainly in the case of modified antennas MOD1 and MOD2 placed on extruded polystyrene STYR.

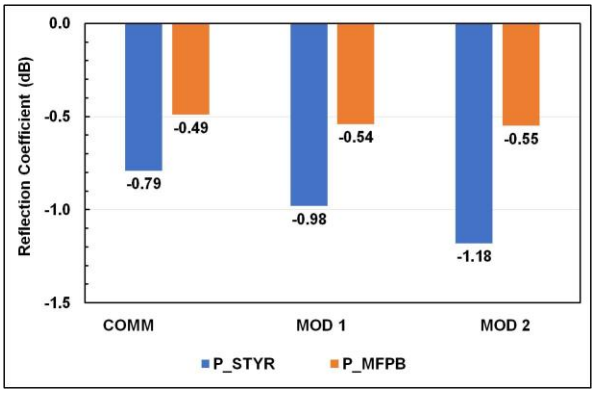

Fig. 6: Measured reflection coefficient of the commercial antenna COMM and modified antennas MOD1 and MOD2 printed on paper P, placed on extruded polystyrene STYR (blue columns) and particle board HFPB (orange columns) at 865 MHz frequency.

Measurement of communication quality of passive UHF RFID tags

Passive tags do not have their own power source as compared to the active tags, so they use the energy of electromagnetic waves sent by the reader to generate a response. There are many factors that are a detriment to RFID tag readability, especially in the packaging and distribution environment. Tagging shipped goods for tracking through distribution is becoming a more common practice (Sorrells 2005).

The communication quality of experimental passive UHF RFID tags was assessed at 865 MHz frequency by measuring the distance of the tag from the antenna of the reader required for identification of the electronic product code EPC (Electronic Product Code), for reading and recording data into the user memory of the NXP UCODE G2iM+ chip. When measuring the communication quality, the tags were placed on the background materials (paperboard PB2, extruded polystyrene board STYR or particle board MFPB). Since in real conditions, tags are mainly placed on packaging, which can be made of different types of paper, cardboard, plastic and wood.

The results of measuring the communication quality of passive UHF RFID tags TCOMM_P, TMOD1_P and TMOD2_P with printed aluminum antennas on 75 μm thick paper P, with relative electrical permittivity of 2.8, are shown in Fig. 7 and tags TCOMM_PB1, TMOD1_PB1 and TMOD2_PB1 with printed antennas on 290 μm thick paperboard PB1 in Fig. 8.

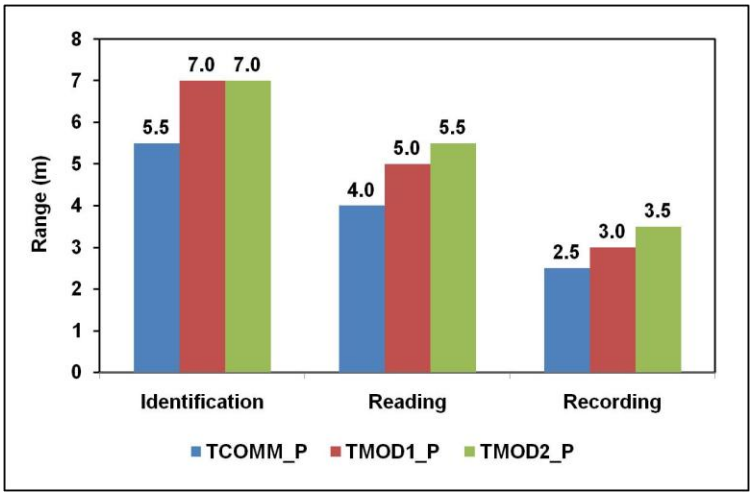

Fig. 7: Communication quality of passive UHF RFID tags TCOMM_P, TMOD1_P, TMOD2_P at 865 MHz frequency (Tags are placed on 1 mm thick paperboard PB2).

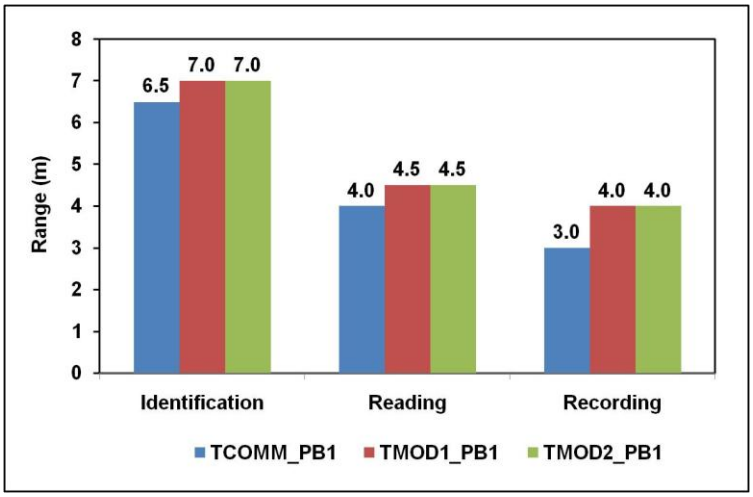

Fig. 8: Communication quality of passive UHF RFID tags TCOMM_PB1, TMOD1_PB1, TMOD2_PB1 at 865 MHz frequency (Tags are placed on 1 mm thick paperboard PB2).

The tags were placed during the measurement on the paperboard PB2, which has relative electrical permittivity of 3.5 and a thickness of 1 mm. Communication quality of passive UHF RFID tags with modified antennas MOD1 and MOD2 printed on both substrates improved compared to tags TCOMM_P and TCOMM_PB1 (with a commercial COMM antenna), identification range of tags TMOD1_P and TMOD2_P by 27%, tags TMOD1_PB1 and TMOD2_PB1 by 8%, reading range of tag TMOD1_P by 25% and tag TMOD2_P by 38%, tags TMOD1_PB1 and TMOD2_PB1 by 12.5%, recording range of tag TMOD1_P by 20% and tag TMOD2_P by 40%, tags TMOD1_PB1 and TMOD2_PB1 by 33%. The reading range of tags with modified MOD1 and MOD2 antennas printed on paper P was greater as compared to modified tags printed on paperboard PB1.

Figs. 9 and 10 present the results of measuring the communication quality of passive UHF RFID tags TCOMM_P, TMOD1_P, TMOD2_P and TCOMM_PB1, TMOD1_PB1,

TMOD2_PB1, placed on 40 mm thick extruded polystyrene STYR with relative electrical permittivity 2.4.

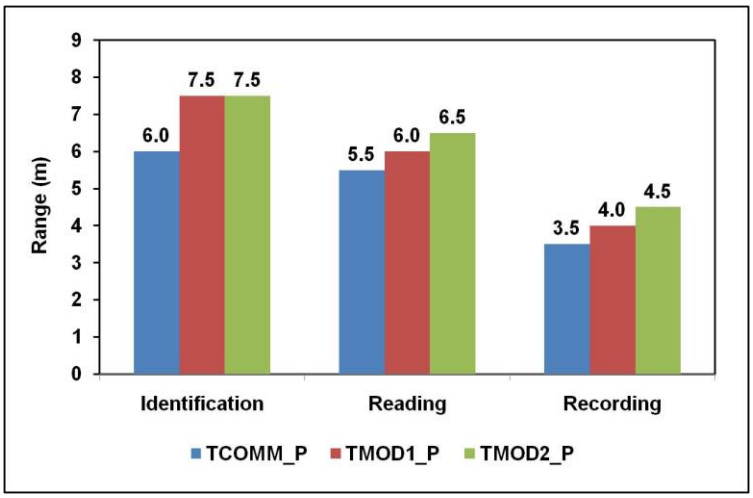

Fig. 9: Communication quality of passive UHF RFID tags TCOMM_P, TMOD1_P, TMOD2_P at 865 MHz frequency (tags are placed on 40 mm thick extruded polystyrene STYR).

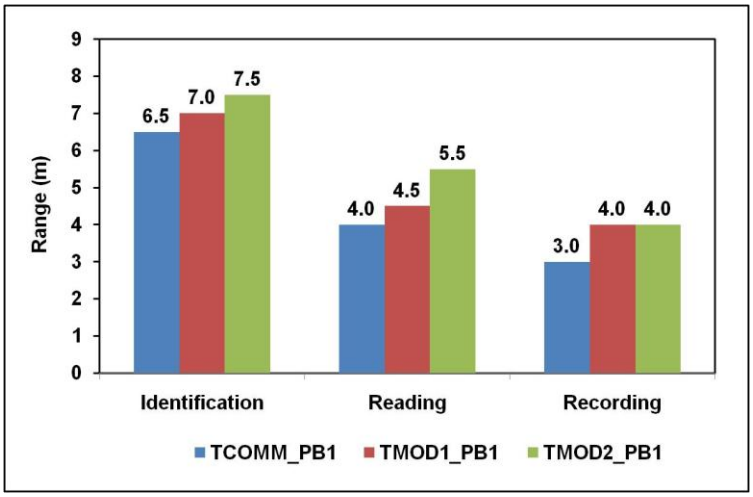

Fig. 10: Communication quality of passive UHF RFID tags TCOMM_PB1, TMOD1_PB1, TMOD2_PB1 at 865 MHz frequency (tags are placed on 40 mm thick extruded polystyrene STYR).

Communication quality of tags with modified antennas MOD1 and MOD2 printed on both substrates improved compared to tags TCOMM_P and TCOMM_PB1 (with a commercial COMM antenna), identification range of tags TMOD1_P and TMOD2_P by 25%, tag TMOD1_PB1 by 7% and tag TMOD2_PB1 by 15%, reading range of tag TMOD1_P by 9% and tag TMOD2_P by 18%, tag TMOD1_PB1 by 12% and tag TMOD2_PB1 by 38%, recording range of tag TMOD1_P by 14% and tag TMOD2_P by 29%, tags TMOD1_PB1 and TMOD2_PB1 by 33%.

Passive UHF RFID tags TCOMM_P, TMOD1_P, TMOD2_P with antennas printed on paper had a significantly greater reading range (5.5-6.5 m) compared to tags TCOMM_PB1, TMOD1_PB1, TMOD2_PB1 with antennas printed on paperboard, which had a reading range

of 4 - 5.5 m. The reading range of tags TCOMM_P, TMOD1_P, TMOD2_P placed on extruded polystyrene STYR (Fig. 9) as well as on paperboard PB2 was the same (Fig. 8).

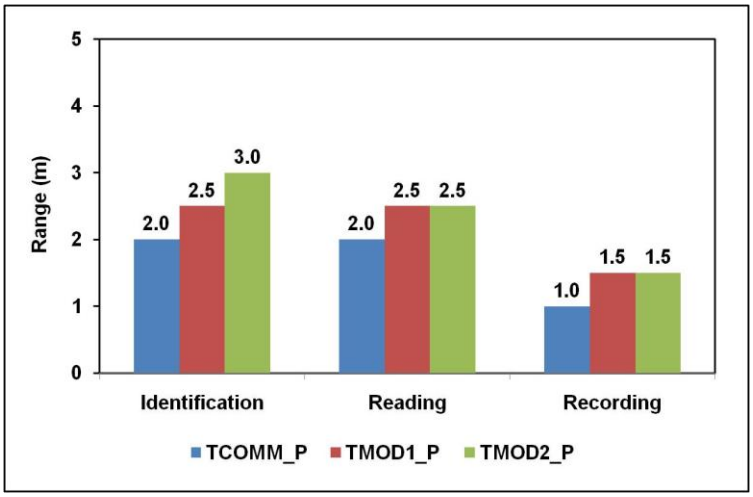

Fig. 11: Communication quality of passive UHF RFID tags TCOMM_P, TMOD1_P, TMOD2_P at 865 MHz frequency (Tags are placed on 38 mm thick particle board MFPB).

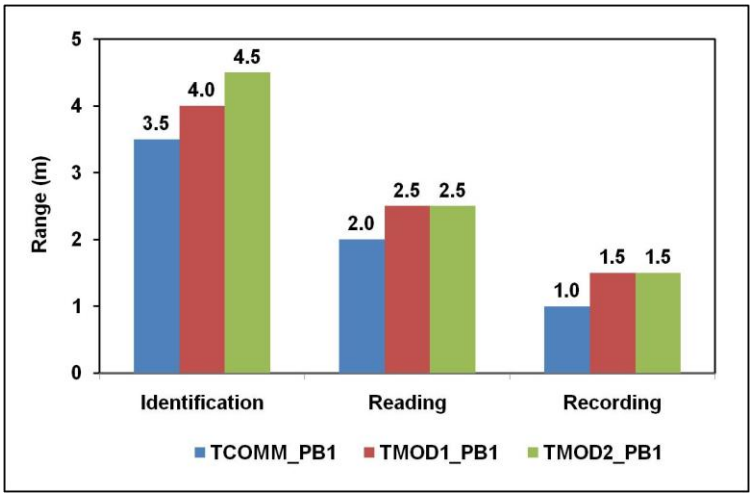

Fig. 12: Communication quality of passive UHF RFID tags TCOMM_PB1, TMOD1_PB1, TMOD2_PB1 at 865 MHz frequency (Tags are placed on 38 mm thick particle board MFPB).

Figs. 11 and 12 show the results of measuring the communication quality of passive UHF RFID tags TCOMM_P, TMOD1_P, TMOD2_P and TCOMM_PB1, TMOD1_PB1, TMOD2_PB1, placed on particle board MFPB, which has relative electrical permittivity of 6.7 and a thickness of 38 mm. Communication quality of tags with modified antennas MOD1 and MOD2 printed on both substrates improved compared to tags TCOMM_P and TCOMM_PB1 (with a commercial COMM antenna), identification range of tag TMOD1_P by 25% and TMOD2_P by 50%, tag TMOD1_PB1 by 14% and tag TMOD2_PB1 by 29%, reading range of tags TMOD1_P and TMOD2_P by 25%, tags TMOD1_PB1 and TMOD2_PB1 by 25%, recording range of tags TMOD1_P and TMOD2_P by 50%, tags TMOD1_PB1 and TMOD2_PB1 by 50%.

The identification range 3.5-4.5 m of passive UHF RFID tags TCOMM_PB1, TMOD1_PB1, TMOD2_PB1 was significantly greater (Fig. 12) compared to the identification range 2-3 m of tags TCOMM_P, TMOD1_P, TMOD2_P (Fig. 11). We assume that this positive effect is caused by covering the particle board MFPB with paperboard PB1 with relative electrical permittivity 3.3, which is 4 times thicker compared to paper P.
The communication quality of passive UHF RFID tags placed on particle board MFPB is lower when compared to tags placed on paperboard PB2 as well as extruded polystyrene STYR. The reason for the lowest communication quality of the tags placed on the particle board MFPB is the highest relative electrical permittivity of the background material (Tab. 1).

CONCLUSIONS

The simulation software SONNET was used to modify the design of the commercial UHF RFID antenna and calculate the simulated reflection coefficients of the antennas. Two modified antennas were prepared by simulation, which had lower reflection coefficients at resonance frequency than the commercial antenna.

A comparison of the measured reflection coefficients of antennas printed on paper, placed on extruded polystyrene and particle board at 865 MHz frequency shows that antennas placed on extruded polystyrene had a lower reflection coefficient than antennas placed on particle board. The reason is lower relative electrical permittivity of extruded polystyrene 2.4 than particle board 6.7. The positive effect of the design of modified antennas was manifested especially when placed on extruded polystyrene.

The communication quality of passive UHF RFID tags prepared by connecting the memory chip NXP UCODE G2iM+ to printed antennas on paper and paperboard was determined at 865 MHz frequency. When measuring communication quality, tags were placed on thicker paperboard, extruded polystyrene and particle, because in practice, tags are most often placed on packaging made of the mentioned materials.

The communication quality of passive UHF RFID tags with modified antennas was better than tags with commercial antennas printed on paper and paperboard and placed on all background materials. Tags placed on thicker paperboard and extruded polystyrene had better communication quality compared to tags placed on particle board, which is related to its higher relative electrical permittivity.

Passive UHF RFID tags with antennas printed on paper, placed on extruded polystyrene had a significantly greater reading range (5.5-6.5 m) compared to tags with antennas printed on paperboard (4 - 4.5 m). The reading range of tags with antennas printed on paperboard placed on thicker paperboard was the same as on extruded polystyrene.

Passive UHF RFID tags with antennas printed on paperboard placed on particle board had a significantly greater identification range of 3.5 - 4.5 m than tags with antennas printed on paper placed on particle board 2 - 3 m. We assume that this effect is caused by covering the particle board with paperboard, which has two times lower relative electrical permittivity (3.3) than particle board (6.7) and four times greater thickness than paper.

ACKNOWLEDGMENT

This work was supported by the Slovak Research and Development Agency under the contract No. APVV-19-0029.

REFERENCES

1. Aliaga, C., Zhang, H., Dobon, A., Hortal, M., Beneventi, D., 2015: The influence of printed electronics on the recyclability of paper: a case study for smart envelopes in courier and postal services. Waste Management 38(1): 41-48.
2. An, K., 2019: High speed nozzle jet printing for bendable organic light emitting diodes. Flexible and Printed Electronics 4(1): 015009.
3. Arazna, A., Janeczek, K., Futera, K., 2017: Mechanical and thermal reliability of conductive circuits inkjet printed on flexible substrates. Circuit World 43(1): 9-12.
4. Bollström, R., Toivakka, M., 2013: Paper substrate for printed functionality. Pp 945-966,15th Fundamental Research Symposium, Cambridge, September 2013.
5. Brodnjak, U.V., Todorova, D., 2017: Novel packaging paper made from blend fillers of chitosan and rice starch. IOSR Journal of Polymer and Textile Engineering 4(3): 33-43.
6. Fedeli, A., Pastorino, M., Raffetto, M., Randazzo, A., 2017: 2-D Green's function for scattering and radiation problems in elliptically layered media with PEC cores. IEEE Transactions on Antennas and Propagation 65(12): 71107118.
7. Gao, B., Yuen, M.F., 2008: Pasive UHF RFID with ferrite electromagnetic band gap (EBG) material for metal objects tracking. Pp 1990-1994, 58th Electronic Components and Technology Conference, 27-30 May, Like Buena Vista, Florida.
8. García, E., Delgado, C., Lozano, L., Cátedra, F., 2019: An efficient strategy for parallelisation of multilevel fast multipole algorithm using CUDA. IET Microwaves, Antennas & Propagation 13(10): 1554-1563.
9. Geyer, R., Jambeck, J.R., Law, K.L., 2017: Production, use, and fate of all plastics ever made. Science Advanced 3(7): e1700782.
10. Gigac, J., Fišerová, M., 2022: Effect of smoothing in calender and hot stamping machine on the properties of coated paperboards for printed electronics. Wood Research 67(1): 26-40.
11. Gigac, J., Stankovská, M., Fišerová, M., 2018: Improvement of oil and grease resistance of cellulosic materials. Wood Research 63(5): 871-886.
12. Glogic, E., Futsch, R., Thenot, V., Iglesias, A., Joyard-Pitiot, B., Depres, G., Rougier, A. Sonnemann, G., 2021: Development of eco-efficient smart electronics for anticounterfeiting and shock detection based on printable inks. ACS Sustain. Chemical Engineering 9(35): 11691-11704.
13. Griffin, J., Durgin, G., Kippelen, B., 2005: Radio link budgets for 915 MHz RFID antennas placed on various objects. Pp 22 -26, Texas Wireless Symposium.
14. He, H., Sydänheimo, L., Virkki, J., Ukkonen, L., 2016: Experimental study on inkjet-printed passive UHF RFID tags on versatile paper-based substrates. International Journal of Antennas and Propagation 2016(9): 1-8.

15. Chin, K.C., Tsai, C.H., Chang, L.C., Wei, C.L., Chen, W.T., Chen, C.S., Lai, S.J., 2008: Design of flexible RFID tag and rectifier circuit using low cost screen printing process. Pp 1940-1946, IPC, Printed Circuits Expo, Apex and the Designers Summit, April 1-3, Las Vegas, Nevada, USA.
16. Ilyas, R.A., Sapuan, S.M., Ishak, M.R., Zainudin, E.S., Atikah, M.S.N., Hazrol, M.D., Huzaifah, M.R.M., 2018: Water barrier properties of biodegradable films reinforced with nanocellulose for food packaging application: A review. Pp 55-59, 6th Postgraduate Seminar on Natural Fiber Reinforced Polymer Composites, Malaysia.
17. Janeczek, K., 2010: Performance of RFID tag antennas printed on flexible substrates. Pp 345-348. XII International PhD Workshop OVD 2010, Poland.
18. Kaur, P., Aggarwal, S.K., De, A., 2015: A survey of techniques used for performance enhancement of patch Antenna using metamaterials. IOSR Journals of Electronics and Communication Engineering 10(6): 98-109.
19. Kavčič, U., Pivar, M., Dokič, M., Svetec, D. G., Pavlovič, L., Muck, T., 2014: UHF RFID tags with printed antennas on recycled papers and cardboards. Materials and technology 48(2): 261-267.
20. Kim, Y.Y., Yang, T.Y., Suhonen, R., Välimäki, M., Maaninen, T., Kemppainen, A., Jeon, N.J., Seo, J., 2019: Gravure-printed flexible perovskite solar cells: toward roll-to-roll manufacturing. Advanced Science 6(7): 1802094.
21. Kopačič, S., Walzl, A., Zankel, A., Leitner, E., Bauer, W., 2018: Alginate and chitosan as a functional barrier for paper-based packaging materials. Coatings 8(7): 235-241.
22. Lakafosis, V., Rida, A., Vyas, R., Yang, L. Nikolaou, S., Tentzeris, M.M., 2010: Progress towards the first wireless sensor networks consisting of nkjet-printed, paper-based RFID-enabled sensor tags. Proceedings of the IEEE 98, 2010(9): 1601-1609.
23. Li, J., Shrivastava, P., Gao, Z., Zhang, H.C., 2004: Printed circuit board recycling: a state-of-the-art survey. IEEE Transactions on Electronics Packaging Manufacturing 27(1): 33-42.
24. Long, Z., Wu, M., Peng, H., Dai, L., Zhang, D., Wang, J., 2015: Preparation and oil-resistant mechanism of chitosan/cationic starch oil-proof paper. BioResources 10(4): 7907-7920.
25. Merilampi, S., Ukkonen, L., Sydänheimo, L., Ruuskanen, P., Kivikoski, M., 2007: Analysis of silver ink bow-tie RFID tag antennas printed on paper substrates. International Journal of Antennas and Propagation, article ID 90762, 9 pp.
26. Mishra, G., Jha, R., Rao, M.D., Meshram, A., Singh, K.K., 2021: Recovery of silver from waste printed circuit boards (WPCBs) through hydrometallurgical route: A review. Environmental Challanges 4: 100073.
27. Öhlund, T., Andersson, M., 2012: Effect of paper properties on electrical conductivity and pattern definition for silver nanoparticle inkjet ink. Pp 115-119, Proceedings of LOPE-C.
28. Rida, A., Li, Yang, L., Vyas, R., Tentzeris, M.M., 2009: Conductive inkjet-printed antennas on flexible low-cost paper-based substrates for RFID and WSN applications. IEEE Antennas and Propagation Magazine 51(3): 13-23.

29. Salmerón, J.F., Molina-Lopez, F., Briand, D., Ruan, J.J., Rivadeneyra, A., Carvajal, M.A., Capitan-Vallvey, L.F., de Rooij, N.F., Palma, A.J., 2014: Properties and printability of inkjet and screen-printed silver patterns for RFID antennas. Journal of Electronic Materials 43(2): 604-17.
30. Shrestha, K., Kim, Y., Jung, Y., Kim, S., Truong, H., Cho, G.: 2021: Wireless pH-logger label for intelligent food packaging. Flexible and Printed Electronics 6(4): 044001.
31. Sonnier, R., Taguet, A., Ferry, L., Lopez-Cuesta, J.M., 2018: Towards bio-based flame retardant polymers. Part of Springer Briefs in Molecular Science, Springer, Pp 33-72.
32. Sorrells, P., 2005: Optimizing in RFID Systems. Article. ELectronics products, technology, design for engineers and managers. www.ednmag.com. 23 Sept. 2005.
33. Sowade, E., Polomoshnov, M., Willert, A., Baumann, R.R., 2019: Toward 3D-printed electronics: Inkjet-printed vertical metal wire interconnects and screen-printed batteries. Advanced Engineering Materials 21(10): 1900568.
34. Stergiou, C., Eleftheriou, E., Zaspalis, V., 2012: Enhancement of the near-field UHF RFID with ferrite substrates. IEEE Transaction on Magnetics 48(4): 1497-1500.
35. Taggar, K., Gad, E., McNamara, D., 2019: High-order unconditionally stable time-domain finite-element method. IEEE Antennas and Wireless Propagation Letters 18(9): 1775–1779.
36. Taylor, D.H., 2017: The digital print value proposition for thermal transfer: Case study with printed electronics. PFFC-Online "On Press" April 2017.
37. Taylor, D.H., Harrison, D., 2017: High volume digital printing of flexible electronics with continuous copper and aluminium. LOPEC 2017, Munich, March 2017.
38. Wang, X., Zheng, S., Zhou, F., Qin, J., Shi, X., Wang, S., Sun, Ch., Bao, X., Wu, Z.S., 2020: Scalable fabrication of printed Zn/MnO_2 planar micro-batteries with high volumetric energy density and exceptional safety. National Science Review 7(1): 64-72.
39. Wäger, P.A., Eugster, M., Hilty, L.M., Som, C., 2005: Smart labels in municipal solid waste - a case for the precautionary principle? Environment Impact Assessment Review 25(5): 567-86.
40. Zhang, L., Wang, H., Zhao, Y., Guo, Y., Hu, W., Yu, G., Liu, Y., 2013: Substrate-free ultra-flexible organic field-effect transistors and five-stage ring oscillators. Advanced Materials 25(38): 5455-5460.
41. Zhang, B., Tang, X., Zhang, J., Liu, Ch., He, D., Wu, Z.P., 2019: Long read range and flexible UHF RFID tag antenna made of high conductivity graphene-based film. International Journal of RF and Microwave Computer-Aided Engineering 30(1): e21993.
42. Zichner, R., Baumann, R.R., 2011: Communication quality of printed UHF RFID transponder antennas. Pp 361-363, LOPE-C, Messe Frankfurt, Germany.
43. Xi, J., Zhu, H., Ye, T.T., 2011: Exploration of printing-friendly RFID antenna designs on paper substrates. Pp 38-44, IEEE International Conference on RFID.

JURAJ GIGAC*, MÁRIA FIŠEROVÁ, SVETOZÁR HEGYI, MAROŠ KOVÁČ
PULP AND PAPER RESEARCH INSTITUTE
DÚBRAVSKÁ CESTA 14
841 04 BRATISLAVA
SLOVAK REPUBLIC
*Corresponding author: gigac@vupc.sk